ADVANCED MATERIALS INTERFACES
Open Access
www.advmatinterfaces.de

Highly Efficient Luminescent Solar Concentrators Based on BODIPY Derivatives

Antonino Arrigo, Chiara Maria Antonietta Gangemi,* Anna Barattucci, Paola Maria Bonaccorsi, Valentina Greco, Alessandro Giuffrida, Salvatore Genovese, Sebastiano Campagna,* Francesco Nastasi, and Fausto Puntoriero*

Three new chromophores based on difluoroborondipyrromethene dyes (Bodipy-1, Bodipy-2, and Bodipy-3) are used as precursors to prepare luminescent solar concentrators (LSC) based on poly-acrylate, following a thermally activated polymerization involving lauryl methacrylate as monomer, ethyl glycol dimethacrylate as cross-linking agent, and lauroyl peroxide as initiator. The new dyes exhibit typical BODIPY absorption and emission properties in dichloromethane fluid solution, assigned to the lower-lying singlet π–π^* level, which in the case of Bodipy-2 and Bodipy-3, both containing diamino-substituted styryl subunits in their structure, has a strong charge transfer contribution. The LSCs obtained starting from each of the three Bodipys are interfaced to silicon photovoltaic (PV) cells, and the PV light-to-energy conversion efficiencies η_{opt} for the three systems are calculated. The results yield η_{opt} of 4.53% for LSC-Bodipy-1, 5.26% for LSC-Bodipy-2, and 8.23% for LSC-Bodipy-3. The optical efficiency for LSC-Bodipy-3 is a remarkable value among the LSC based on organic dyes.

1. Introduction

To solve the increasing problem of sustainable energy needs, it is necessary to develop renewable, safe, and efficient energy sources.[1] Among these, the production of electricity using sunlight is one of the most significant, considering that every hour the earth's surface receives from the sun a quantity of energy approximately equal to the energy consumed by the planet during 1 year.[2,3] Several technologies for solar energy conversion are available, and in the last decades, photovoltaic (PV) cells have been developed, achieving excellent conversion efficiencies. Nevertheless, to satisfy the human energy need, some habitable landscapes would need to be covered by the existing silicon solar panels, implying many environmental and strategic issues.[4] As a promising implementation, the research is focusing on new technologies able to increase the efficiency and/or the integration of photovoltaic devices into buildings, leading us to consider applications on facades.[5] In this field, luminescent solar concentrators, LSCs, have been identified as a promising technology. LSCs can be made using glass, as well as polymeric matrices, containing chromophores embedded in the solid matrix. When LSC is exposed to solar irradiation, the chromophore is photoexcited and its luminescence is then guided (due to total internal reflection) to the edges of the slab, where it is converted into electricity by PV panels positioned at the borders of the LCS.[6] Such LSC-PV devices can be integrated as windows in architectural structures (thus producing energy without significantly altering the indoor illumination, provided that the chromophores exclusively absorb in the UV and/or NIR region), and this is an advantage compared to photovoltaics panels that can be applied only on the rooftops, especially when the rooftop is too small to accommodate PV devices necessary for the energy need of towers or tall buildings.[7,8]

A crucial aspect influencing the LSC final performance is the selection of the chromophore which should have specific characteristics, such as i) a high molar extinction coefficient throughout all the solar spectrum (however, for reducing the impact on indoor illumination, the absorption should be possibly limited to UV and NIR region) and luminescence quantum yield;

A. Arrigo, S. Genovese, S. Campagna, F. Nastasi, F. Puntoriero
Department of Chemical
Biological
Pharmaceutical and Environmental Sciences, and Interuniversitary
Research Center for Artificial Photosynthesis
(Solar Chem, Messina Node)
University of Messina
V. F. Stagno d'Alcontres 31, Messina 98166, Italy
E-mail: antonino.arrigo@unime.it; campagna@unime.it

C. M. A. Gangemi, A. Barattucci, P. M. Bonaccorsi
Department of Chemical
Biological
Pharmaceutical and Environmental Sciences
University of Messina
V.le F. Stagno d'Alcontres 31, Messina 98166, Italy
E-mail: chiaramariaantonietta.gangemi@unime.it

V. Greco, A. Giuffrida
Department of Chemical Sciences
University of Catania
Viale A. Doria 6, Catania 95100, Italy

The ORCID identification number(s) for the author(s) of this article can be found under https://doi.org/10.1002/admi.202400114

DOI: 10.1002/admi.202400114

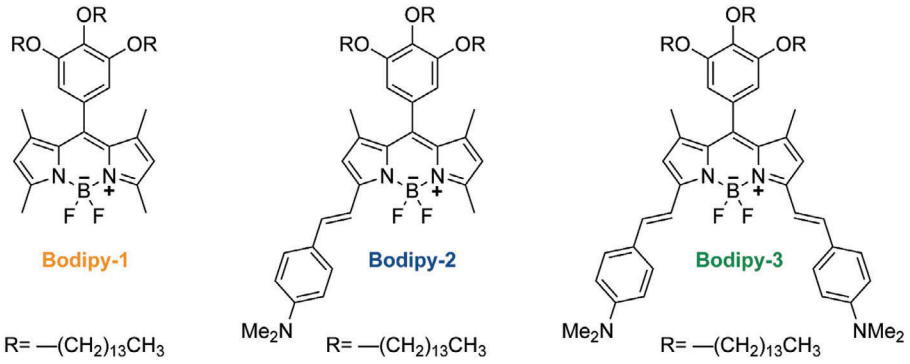

Figure 1. Molecular structure of the newly synthesized BODIPY derivatives.

ii) photostability; iii) large Stokes shift; iv) easy tunability of the luminescence; and v) low toxicity.[9]

Many luminophores, either molecules or semiconductor quantum dots,[10] have been used in LSCs, achieving high values of solar-to-energy efficiencies; for a long time, the record power conversion efficiency for an LSC-PV cell has been around 7.1% reached in 2008 using a combination of two organic dyes in an LSC coupled to GaAs cells;[11] recently, K. Kim et al. reported the highest value of power conversion efficiency present in literature (up to our knowledge) that is 9.6% using LSC-PVs based on up-conversion dual panel LSCs and perovskite solar cells (PSCs).[12]

Inspired by these results and leafing the library of organic dyes, we focused our attention on the BODIPY (difluoroBOronDIPYrromethene) derivatives, which have extremely intriguing properties[13] (for instance, they exhibit strong visible absorption and impressive luminescence quantum yield, approaching 100%), and had been used in several fields[13b,14–17] including solar energy conversion and LSCs.[18,19]

In this paper, we present the synthesis and photophysical studies on three new BODIPY derivatives (**Figure 1**), exhibiting bright luminescence in the visible region. Such compounds possess three aliphatic groups to facilitate homogeneous dispersion within the polymeric matrix used for the preparation of the LSCs. Two of them (**Bodipy-2** and **Bodipy-3**) have one or two *p*-(*N*,*N*-dimethylamino)-styryl groups in the molecular skeleton, tailored to undergo structural modifications reacting with the radical initiator, used in the multicomponent polymerization process to fabricate the LSC. The product of such reactivity is a mixture of BODIPY derivatives, produced during the fabrication of LSC and entrapped in the polymeric matrix, which was expected to lead to higher-performant devices for solar-to-energy conversion, due to a larger overlap with the solar spectrum. Indeed, the optical efficiency calculated for the **LSC-Bodipy-3** system is 8.23%, which is a remarkable value among the LSC doped with dyes reported in the literature.

2. Results and Discussion

2.1. Synthesis of BODIPY Species and Photochemical Characterization in Solution

3,4,5-Tris(tetradecyloxy)benzoyl chloride (**3**, see Scheme S1, Supporting Information), obtained following literature procedures,[20] was reacted with 2,4-dimethyl-pyrrole and $BF_3{\cdot}Et_2O$ to afford **Bodipy-1**, in moderate yield.[21] **Bodipy-1** was converted into **Bodipy-2** and **Bodipy-3**, in a ratio of 4/6, respectively, through a Knoevenagel condensation with 4-(dimethylamino) benzaldehyde.[22] **Bodipy-2** can be easily separated by column chromatography and further converted into **Bodipy-3** (Scheme S1, Supporting Information). The three Bodipy derivatives were purified and completely characterized by ^{1}H-NMR and ^{13}C-NMR.

The absorption spectrum of **Bodipy-1** in dichloromethane (DCM) solution is dominated by an intense band centered at around 500 nm, attributable to $\pi \rightarrow \pi^*$ transitions (see **Figure 2**). The introduction of one or two *p*-(*N*,*N*-dimethylamino)-styryl groups leads to a substantial modification of the spectral profile. Indeed, **Bodipy-2** exhibits a red-shifted and less structured absorption band with respect to **Bodipy-1**. This effect is attributable to the presence of the styryl fragment which extends the delocalization of the π system and to the presence of the peripheral amino group which introduces a charge transfer character, where the HOMO is centered on the dimethylamino fragment and the LUMO on the delocalized structure of the BODIPY "core." Such behavior is amplified in the case of **Bodipy-3**, due to the presence of two donor substituents and an even more extensive delocalization offered by the two styryl groups (Figure 2).

In DCM fluid solution, **Bodipy-1** exhibits luminescence from an excited state centered on the borondipyrrole core, while in the case of **Bodipy-2** and **Bodipy-3**, the emission bands are wider and shifted to lower energy (Figure 2). In both these latter cases, the luminescence comes from excited states with charge transfer character. It is interesting to highlight that passing from **Bodipy-1** to **Bodipy-3**, the Stokes-shift increases along the series.

For all the investigated species, the excited state decay is mono-exponential with lifetimes in the nanoseconds timescale. **Bodipy-1** has a luminescence quantum yield of 0.82 while **Bodipy-2** and **Bodipy-3** have a lower value (0.37 and 0.33 respectively), in accordance with the presence of the amino groups which trigger the charge transfer transitions. All the absorption and photophysical data are summarized in **Table 1**.

2.2. Fabrication of LSC and Photochemical Studies

Among the existing materials to manufacture the LSCs, we selected poly-acrylates, because they have considerably good transparency and absorb less light than standard window glasses.[23]

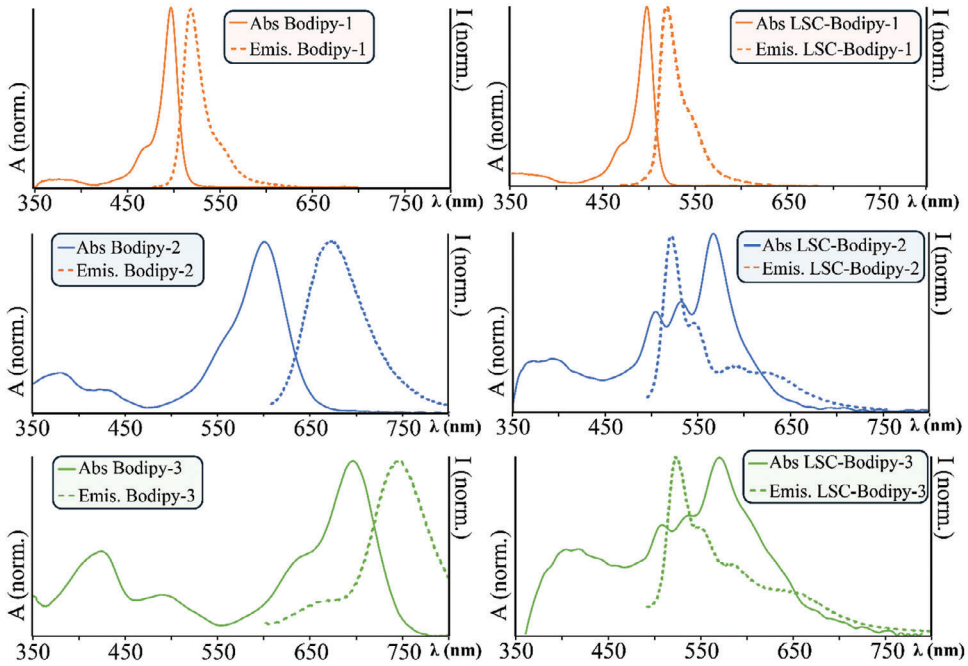

Figure 2. Absorption (solid line) and emission (dashed lines) spectra (λ_{exc} = 470 nm) of **Bodipy-1**, **Bodipy-2**, and **Bodipy-3** in DCM on the left panels and in the LSC on the right panels.

Such a feature is important to avoid absorption of the chromophore luminescence by the matrix, which would negatively affect the LSC performance. Moreover, poly-acrylates LSC have an efficient waveguide: according to Snell's law, up to 75% of the chromophore-emitted light can be concentrated on the edges of the slab by total internal reflection.[24]

The LSCs were produced following a thermally-activated polymerization, involving lauryl methacrylate as the monomer, ethyl glycol dimethacrylate as the cross-linking agent, and lauroyl peroxide as the initiator,[25] in the presence of each BODIPY subunit (BODIPY:initiator typically in ratio 1:6700, details in Supporting Information). This procedure was repeated several times, using different concentrations of BODIPYs and keeping the concentration of initiator constant (from ratio 1:6700 to 1:1700 of BODIPY:initiator), but detecting always the same final products, on the basis of their absorption and emission properties. In fact, the composition of the final mixture is independent of the amount of BODIPY in our experimental conditions, probably because the amount of BODIPY in all preparations we used is always in severe stoichiometric defect with respect to the amounts of monomer and initiator.

The resulting LSCs are transparent, slightly colored, and show intense BODIPY's luminescence from the edges under UV irradiation of the top surface (**Figure 3**). Details of the dimension and optical properties of the prepared LSCs are given in the Supporting Information (Table S1, Supporting Information).

Table 1. Absorption and photophysical properties of **Bodipy-1**, **Bodipy-2**, and **Bodipy-3** in DCM and in LSC matrix.

		Absorption		Luminescence		
		λ_{max} [nm]	ε (M^{-1} cm^{-1})	λ_{max} [nm]	φ	τ [ns]
Bodipy-1	in DCM	498	75 000	512	0.82	4.5
	in LSC	496	–	518	–	5.2
Bodipy-2	in DCM	601	112 600	669	0.37	3.7
	in LSC	567	–	515	–	5
Bodipy-3	in DCM	696	115 000	746	0.33	2.4
	in LSC	575	–	521	–	4.3

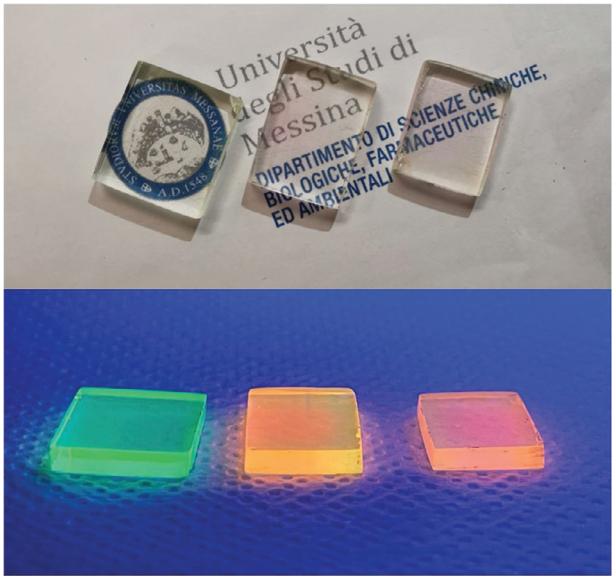

Figure 3. From left to right, **LSC-Bodipy-1**, **LSC-Bodipy-2**, and **LSC-Bodipy-3** before and after UV irradiation at 365 nm.

Comparing the absorption spectra of **Bodipy-1** in DCM and LSC, the absorption maximum red-shifts of about 2 nm (from 496 to 498 nm); this effect is attributed to the different chemical environments.

However, comparing solution versus rigid matrix phase, the absorption spectra of **Bodipy-2** and **Bodipy-3** show significant changes: the visible absorption maximum shifts from 601 to 567 nm for **Bodipy-2**, and from 696 to 575 nm for **Bodipy-3** (Figure 2 and Table 1) and other two bands appear at higher energy.

It should be taken into account that the initiator is able to attack the styryl double bond,[26] thus generating a mixture of Bodipy derivatives, in the skeleton of which the electronic communication between the dipyrrole core and the arylamino fragment is interrupted. The formation of these derivatives was supported by absorption spectroscopy (see Supporting Information).

The fraction of absorbed photons over the solar spectrum ($\eta_{\text{abs-vis}}$), has been calculated as the ratio between the area of each transmission spectrum of LSC-Bodipy species, subtracted from the area of the solar spectrum from 370 to 1050 nm, and the area of the solar spectrum (**Figure 4**). The values of $\eta_{\text{abs-vis}}$ are 26.8% for **LSC-Bodipy-1**, 21.7% for **LSC-Bodipy-2**, and 26.2% for **LSC-Bodipy-3**. It is worth noting that the $\eta_{\text{abs-vis}}$ for the blank LSC is 14.3% which is not negligible, considering some incident light trapped in the waveguide of the rigid matrix.

The emission spectrum of **Bodipy-1** in LSC, related to the radiative $\pi^* \rightarrow \pi$ transition, is slightly red-shifted compared to the solution phase (Table 1 and Figure 2). The emission spectra of **LSC-Bodipy-2** and **LSC-Bodipy-3** display the contribution of the various derivatives obtained during the polymeric matrix preparation. As a matter of fact, the luminescence profiles appear blue-shifted compared to ones exhibited by the dyes in the solution phase and are both dominated by a band in the range 510–525 nm, which is similar to that of **LSC-Bodipy-1**. This band can be attributed to the radiative deactivation of the excited state of reacted **Bodipy-2** and **Bodipy-3**, where the electronic communication between the dipyrrole core and the arylamino fragment is interrupted. The less intense emission bands observed at longer wavelengths in the emission spectra of **LSC-Bodipy-2** and **LSC-Bodipy-3** can be attributed to the emission contribution of other minor derivatives present in the mixture. The emission spectra of **LSC-Bodipy-2** and **LSC-Bodipy-3** shown in Figure 2 are therefore due to a blend of chromophores. These attributions are substantially supported by comparison with data obtained from the study of intermediates prepared in solution (see Supporting Information).

2.3. Photovoltaic Performance of the LSC-PV Device

To investigate the photovoltaic performances of the device, one edge of the LSC was placed in contact with the silicon PV cell, while the other edges were uncovered, and the slab was irradiated perpendicularly at 100 mW cm^2 using an AM 1.5G solar simulator.[27] During the experiment, the short-circuit current intensity (mA) was detected and converted into short-circuit current density J (mA cm^{-2}), so to take into account the area of the

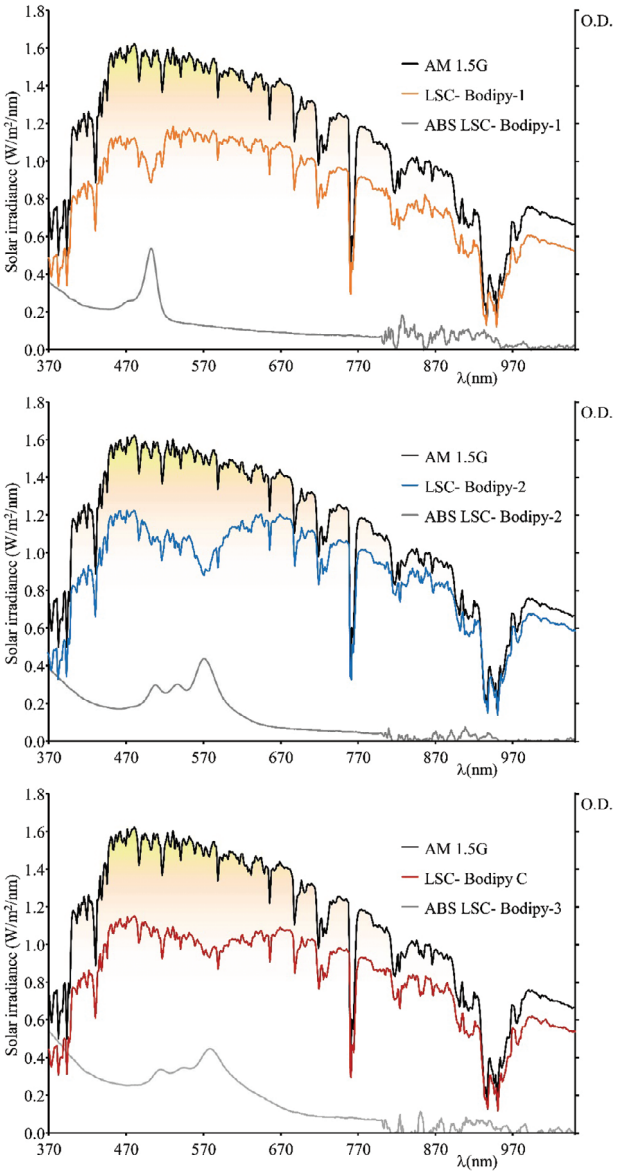

Figure 4. The black spectrum in each panel is the solar spectrum using the AM 1.5G filter. The absorption spectra of LSC-BODIPY systems are grey-coloured. Lines colored in orange for **LSC-Bodipy-1**, blue for **LSC-Bodipy-2**, and red for **LSC-Bodipy-3** represent the spectrum of transmitted AM1.5 light, through LSCs.

LSC in contact with the PV cell. Then, the J values were used to calculate the optical efficiency η_{opt} of the LSC-PV, defined by Equation (1)[25,28,29]

$$\eta_{\text{opt}} = \frac{J_{\text{LSC}}}{J_{\text{PV}} \times G} \quad (1)$$

where J_{LSC} is the short-circuit current density (mA cm^{-2}) of the PV cell coupled with the LSC-Bodipy species; J_{PV} is the short-circuit current density (mA cm^{-2}) of the PV cell obtained by dividing the current intensity by the area of the PV cell directly exposed to the light from AM 1.5G solar simulator;[30] in our case,

Table 2. Photovoltaic data of the LSC blank and with the BODIPY species.

LSC	I [mA]	J_{LSC} [mA cm^{-2}]	G factor	η_{opt} [%]	FF	$\eta_{opt\ abs}$ [%]
Blank	0.10	0.15	1.29	2.38	0.63	–
Bodipy-1	0.16	0.28	1.27	4.53	0.61	36.18
Bodipy-2	0.15	0.32	1.23	5.26	0.63	70.86
Bodipy-3	0.21	0.51	1.26	8.23	0.64	69.04

The results reported are average values of three experiments. The concentration of **Bodipy-1**, **Bodipy-2**, and **Bodipy-3** in the LSC has been the same so the comparison is possible. FF is the fill factor of the PV device.

J_{PV} is 4.95 mA cm^{-2}; and G is a geometrical factor, defined by Equation (2)[31]

$$G = \frac{A_{top}}{2A_{edgelong} \times 2A_{edgeshort}} \quad (2)$$

where A_{top} is the area of the top surface of the LSC; $A_{edge\ long}$ and $A_{edge\ short}$ are the areas of the long and short edges of the slab, respectively. The G factor is higher for large LSCs than for small ones, and its scope is to bring into account the LSCs geometry in Equation (1), counter-balancing the J_{LSC} which is typically higher for larger LSCs.

The results, summarized in **Table 2**, show η_{opt} of 4.53% for **LSC-Bodipy-1**, 5.26% for **LSC-Bodipy-2**, and 8.23% for **LSC-Bodipy-3**. They suggest that Bodipy-2 in **LSC-Bodipy-2** and Bodipy-3 in **LSC-Bodipy-3** and their derivatives, obtained during the polymeric matrix preparation and there entrapped, contribute to enhancing the solar-to-energy efficiency of the LSC-PV device. Indeed, such a combination of BODIPY derivatives covers a wider range in the absorption and emission spectra with respect to **LSC-Bodipy-1** (see Figure 2).

The same experiment was repeated for the blank sample as well, where some incident light is trapped in the waveguide and arrives at the PV cell, giving a contribution to the photocurrent which cannot be neglected. Such a value (that is 2.38% in our case) can be subtracted from the η_{opt} of the LSC-BODIPY derivatives to remove the contribution of the incident light. Therefore, we could estimate the real optical efficiency of the LSC-PV device: 2.15% for **LSC-Bodipy-1**, 2.88% for **LSC-Bodipy-2** and 5.85% for **LSC-Bodipy-3**, which clearly spotlights the contribution of BODIPYs' luminescence to the efficiency of the device.

By using the value of η_{opt}, it is interesting to calculate the corrected optical efficiency $\eta_{opt,abs}$ according to Equation (3), in order to take into account the fraction of photons absorbed by the LSC-BODIPY device

$$\eta_{opt\ abs}\ \% = \frac{\eta_{opt}}{\eta_{abs-vis\ (LSC-Bodipy)} - \eta_{abs-vis\ (BLANK)}} \quad (3)$$

In Equation (3) $\eta_{abs\ -\ vis\ (LSC\ -\ Bodipy)}$ is the fraction of photons absorbed by the LSC-BODIPY system and $\eta_{abs\ -\ vis\ (BLANK)}$ is the fraction of photons absorbed by the blank LSC. The calculated values of corrected optical efficiency $\eta_{opt,abs}$ are reported in Table 2 where it is possible to note that **LSC-Bodipy-2** has the highest value among this series of devices, mainly due to a lower fraction of photons absorbed compared to **LSC-Bodipy-1** and **LSC-Bodipy-3**.

The optical efficiency of 8.23% for **LSC-Bodipy-3** is an outstanding value for an LSC entrapping an organic dye up to our knowledge. However, the long-term photostability issue remains unsolved. Indeed, the photostability tests carried out on these LSCs show that the initial emission spectrum is slightly altered after 24 h irradiation using the AM 1.5G solar simulator (see Supporting Information).

From Table 2, it is evident that the fill factor (FF) of the photovoltaic cell remains identical over the experiments, independently of whether the current is measured for LSC with or without chromophores. In addition, it is worth noting that the comparison of the J–V curve for the LSC-BODIPYs and the J–V curve of the PV panel without LSC (Figure S13, Supporting Information) underlines that the fill factor of the device is not significantly influenced by the presence of the LSC.

Finally, we monitored whether the LSC-PV photovoltaic performance is affected by the position of the irradiation light on the top surface of the slab. In theory, in cases where the chromophore has a large Stokes-shift, the luminescence and the photocurrent should not be altered when the irradiation light is moved from one edge to the other of the LSC top surface. From a practical viewpoint, the emission intensity slightly decreases when the optical path increases for the emission light, and this is mainly due to bulk defects which can cause the loss of some emitted photons over the optical path.[32,33] As a consequence, the current intensity is expected to follow such a trend. To perform this experiment, we measured the short-circuit current intensity when the light spot (i.e., a 406 nm laser) was moved from one edge to another of the slab surface. The results summarized in **Figure 5** illustrate that the short-circuit current intensity slightly decreases for short distances (this effect occurs in the LSC-Blank as well) and then reaches a plateau, thus testifying to the adequate quality of the device.

3. Conclusions

Three new BODIPY have been used to prepare LSCs, which appeared transparent and slightly colored. Each BODIPY has been designed to have aliphatic chains, to make them soluble within the polymeric matrix used for the preparation of the LSCs. Moreover, two of them (**Bodipy-2** and **-3**) possess styryl groups which makes them subject to the radical attack by the thermal initiator during the polymerization reaction for the LSC fabrication. As a consequence of such a reaction, the LSC-BODIPY contains a combination of BODIPY derivates (as characterized by mass spectroscopy and UV/vis absorption spectroscopy). Thanks to this mixture of fluorophores, **LSC-Bodipy-2** and **-3** have high values of solar-to-energy conversion efficiencies, especially **LSC-Bodipy-3** reaches the value of 8.23% optical efficiency—to the best of our knowledge a notable value when organic dyes are employed—even if the photostability of such devices still needs to be improved.

The results underline that mixing chromophores or even generating a combination of them while preparing the LSC matrix can boost the efficiencies of these devices.

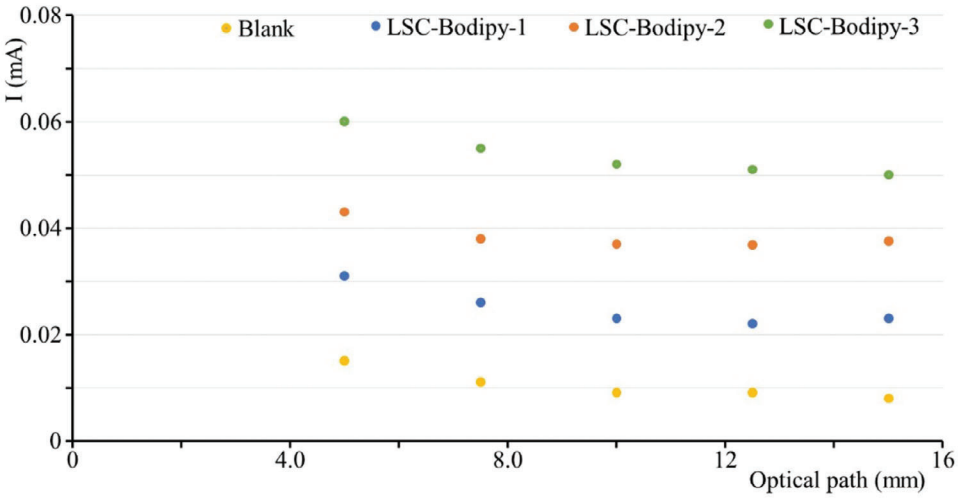

Figure 5. Short-circuit current intensity measured upon excitation of the top surface of LSCs as a function of different distances from the edge, using a laser at 406 nm.

Supporting Information

Supporting Information is available from the Wiley Online Library or from the author.

Acknowledgements

This work was funded in part by the European Union (NextGeneration EU), through the MUR-PNRR project SAMOTHRACE (ECS00000022) and the European Union-FSE-REACT-EU, PON Research and Innovation 2014–2020 DM.1062/2021.

Conflict of Interest

The authors declare no conflict of interest.

Data Availability Statement

The data that support the findings of this study are available in the supplementary material of this article.

Keywords

BODIPY, luminescent solar concentrators, optical efficiency, organic dyes, photochemistry, photovoltaics

Received: February 8, 2024
Revised: March 8, 2024
Published online: May 20, 2024

[1] a) N. Armaroli, V. Balzani, N. Serpone, *Powering Planet Earth: Energy Solutions for the Future*, Wiley-VCH, Weinheim **2013**; b) T. J. Meyer, M. V. Sheridan, B. D. Sherman, *Chem. Soc. Rev.* **2017**, *46*, 6148; c) D. D. Dogutan, D. G. Nocera, *Acc. Chem. Res.* **2019**, *52*, 3143; d) S. Campagna, F. Nastasi, G. L. Ganga, S. Serroni, A. Santoro, A. Arrigo, F. Puntoriero, *Phys. Chem. Chem. Phys.* **2023**, *25*, 1504.

[2] I. Statistics, *Key World Energy Statistics*, International Energy Agency, France **2014**.

[3] R. Eisenberg, D. G. Nocera, *Inorg. Chem.* **2005**, *44*, 6799.

[4] L. Zdražil, S. Kalytchuk, M. Langer, R. Ahmad, J. Pospíšil, O. Zmeškal, M. Altomare, A. Osvet, A. Osvet, R. Zbořil, P. Schmuki, C. J. Brabec, M. Otyepka, Š. Kment, *ACS Appl. Energy Mater.* **2021**, *4*, 6445.

[5] a) F. Meinardi, A. Colombo, K. A. Velizhanin, R. Simonutti, M. Lorenzon, L. Beverina, R. Viswanatha, V. I. Klimov, S. Brovelli, *Nat. Photonics* **2014**, *8*, 392; b) W. H. Weber, J. Lambe, *Appl. Opt.* **1976**, *15*, 2299.

[6] B. P. Jelle, C. Breivik, H. D. Røkenes, *Sol. Energy Mater. Sol. Cells* **2012**, *100*, 69.

[7] M. G. Debije, *Adv. Funct. Mater.* **2010**, *20*, 1498.

[8] W. G. J. H. M. van Sark, *Renewable Energy* **2013**,*49*, 207.

[9] I. Papakonstantinou, M. Portnoi, M. G. Debije, *Adv. Energy Mater.* **2021**, *3*, 2002883.

[10] a) R. Mazzaro, A. Vomiero, *Adv. Energy Mater.* **2018**, *8*, 1801903; b) A. Arrigo, A. M. Cancelliere, M. Galletta, A. Burtone, G. Lanteri, F. Nastasi, F. Puntoriero, *Mater. Adv.* **2023**, *4*, 5200; c) F. Mateen, M. Ali, S. Y. Lee, S. H. Jeong, M. J. Ko, S.-K. Hong, *Sol. Energy* **2019**, *190*, 488; d) J. L. Banal, B. Zhang, D. J. Jones, K. P. Ghiggino, W. W. H. Wong, *Acc. Chem. Res.* **2017**, *50*, 49; e) F. Mateen, S. Y. Lee, S.-K. Hong, *J. Mater. Chem. A* **2020**, *8*, 3708; f) O. Essahili, M. Ouafi, O. Moudam, *Sol. Energy* **2022**, *245*, 58.

[11] L. H. Slooff, E. E. Bende, A. R. Burgers, T. Budel, M. Pravettoni, R. P. Kenny, E. D. Dunlop, A. A. Büchtemann, *Phys. Status Solidi RRL* **2008**, *2*, 257.

[12] a) K. Kim, S. K. Nam, J. Cho, J. H. Moon, *Nanoscale* **2020**, *12*, 12426; b) S. Castelletto, A. Boretti, *Nano Energy* **2023**, *109*, 108269.

[13] a) S. Diring, F. Puntoriero, F. Nastasi, S. Campagna, R. Ziessel, *J. Am. Chem. Soc.* **2009**, *131*, 6108; b) R. Ziessel, G. Ulrich, A. Harriman, *New J. Chem.* **2007**, *31*, 496; c) A. Loudet, K. Burgess, *Chem. Rev.* **2007**, *107*, 4891; d) M. Poddar, R. Misra, *Coord. Chem. Rev.* **2020**, *421*, 213462.

[14] a) G. Ulrich, R. Ziessel, A. Harriman, *Angew. Chem., Int. Ed. Engl.* **2008**, *7*, 1184; b) B. Matarranz, G. Fernández, *Chem. Phys. Rev.* **2021**, *2*, 041304; c) P. Kaur, K. Singh, *J. Mater. Chem. C* **2019**, *7*, 11361; d) H.-B. Cheng, X. Cao, S. Zhang, K. Zhang, Y. Cheng, J. Wang, J. Zhao, L. Zhou, X.-J. Liang, J. Yoon, *Adv. Mater.* **2023**, *35*, 2207546.

[15] A. Barattucci, C. M. A. Gangemi, A. Santoro, S. Campagna, F. Puntoriero, P. Bonaccorsi, *Org. Biomol. Chem.* **2022**, *20*, 2742.
[16] T. Papalia, A. Barattucci, S. Campagna, F. Puntoriero, T. Salerno, P. Bonaccorsi, *Org. Biomol. Chem.* **2017**, *15*, 8211.
[17] P. Bonaccorsi, T. Papalia, A. Barattucci, T. M. Salerno, C. Rosano, P. Castagnola, M. Viale, M. Monticone, S. Campagna, F. Puntoriero, *Dalton Trans.* **2018**, *47*, 4733.
[18] a) O. A. Bozdemir, S. Erbas-Cakmak, O. O. Ekiz, A. Dana, E. U. Akkaya, *Angew. Chem.* **2011**, *123*, 11099; b) A. Brzeczek-Szafran, C. J. Richards, V. M. Lopez, P. Wagner, A. Nattestad, *Phys. Status Solidi A* **2018**, *215*, 1800551; c) S. T. Bailey, G. E. Lokey, M. S. Hanes, J. D. M. Shearer, J. B. McLafferty, G. T. Beaumont, T. T. Baseler, J. M. Layhue, D. R. Broussard, Y.-Z. Zhang, B. P. Wittmershaus, *Sol. Energy Mater. Sol. Cells* **2007**, *91*, 67.
[19] a) N. J. L. K. Davis, R. W. MacQueen, S. T. E. Jones, C. Orofino-Pena, D. Cortizo-Lacalle, R. G. D. Taylor, D. Credgington, P. J. Skabarac, N. C. Greenham, *J. Mater. Chem. C* **2017**, *5*, 1952; b) A. Mirloup, P. Retailleau, R. Ziessel, *Tetrahedron Lett.* **2013**, *54*, 4456; c) J. Roncali, *Adv. Energy Mater.* **2020**, *10*, 2001907; d) C. Yang, W. Sheng, M. Moemeni, M. Bates, C. K. Herrera, B. Borhan, R. R. Lunt, *Adv. Energy Mater.* **2021**, *11*, 2003581.
[20] M. Iliş, M. Micutz, I. Pasuk, T. Staicu, V. Cîrcu, *J. Fluorine Chem.* **2017**, *204*, 84.
[21] a) L. Yang, G. Fan, X. Ren, L. Zhao, J. Wanga, Z. Chen, *Phys. Chem. Chem. Phys.* **2015**, *17*, 9167; b) G. Fan, Y.-X. Lin, L. Yang, F.-P. Gao, Y.-X. Zhao, Z.-Y. Qiao, Q. Zhao, Y.-S. Fan, Z. Chen, H. Wang, *Chem. Commun.* **2015**, *51*, 12447.
[22] a) L. J. Patalag, J. Hoche, M. Holzapfel, A. Schmiedel, R. Mitric, C. Lambert, D. B. Werz, *J. Am. Chem. Soc.* **2021**, *143*, 7414; b) G. Li, W. Hu, M. Zhao, W. Zhao, F. Li, S. Liu, W. Huang, Q. Zhao, *J. Mater. Chem. B* **2020**, *8*, 7356.
[23] F. Meinardi, F. Bruni, S. Brovelli, *Nat. Rev. Mater.* **2017**, *2*, 17072.
[24] M. G. Debije, P. P. C. Verbunt, *Adv. Energy Mater.* **2012**, *2*, 12.
[25] R. Mazzaro, A. Gradone, S. Angeloni, G. Morselli, P. G. Cozzi, F. Romano, A. Vomiero, P. Ceroni, *ACS Photonics* **2019**, *6*, 2303.
[26] J. Gierer, E. Yang, T. Reitberger, *Holzforschung* **1996**, *50*, 342.
[27] F. Purcell-Milton, Y. K. Gun'ko, *J. Mater. Chem.* **2012**, *22*, 16687.
[28] C. Yang, H. A. Atwater, M. A. Baldo, D. Baran, C. J. Barile, M. C. Barr, M. Bates, M. G. Bawendi, M. R. Bergren, B. Borhan, C. J. Brabec, S. Brovelli, V. Bulović, P. Ceroni, M. G. Debije, J.-M. Delgado-Sanchez, W.-J. Dong, P. M. Duxbury, R. C. Evans, S. R. Forrest, D. R. Gamelin, N. C. Giebink, X. Gong, G. Griffini, F. Guo, C. K. Herrera, A. W. Y. Ho-Baillie, R. J. Holmes, S.-K. Hong, T. Kirchartz, et al., *Joule* **2022**, *6*, 8.
[29] Y. Zhous, D. Benetti, Z. Fan, H. Zhao, D. Ma, A. O. Govorov, A. Vomiero, F. Rosei, *Adv. Energy Mater.* **2016**, *6*, 1501913.
[30] H. Zhao, D. Benetti, L. Jin, Y. Zhou, F. Rosei, A. Vomiero, *Small* **2016**, *38*, 5354.
[31] M. Aghaei, R. Pelosi, W. W. H. Wong, T. Schmidt, M. G. Debije, A. H. M. E. Reinders, *Prog. Photovoltaics Res. Appl.* **2022**, *30*, 726.
[32] G. Griffini, M. Levi, S. Turri, *Renewable Energy* **2015**, *78*, 288.
[33] I. Coropceanu, M. G. Bawendi, *Nano Lett.* **2014**, *14*, 4097.